ACS APPLIED MATERIALS & INTERFACES

Research Article

www.acsami.org

Hydrolytically Stable Thiol−ene Networks for Flexible Bioelectronics

Radu Reit,[†] Daniel Zamorano,[‡] Shelbi Parker,[†] Dustin Simon,[§] Benjamin Lund,[§] Walter Voit,[†,‡,§,∥] and Taylor H. Ware*[,†]

[†]Department of Bioengineering, [‡]Department of Chemistry, [§]Department of Materials Science and Engineering, and [∥]Department of Mechanical Engineering, The University of Texas at Dallas, 800 West Campbell Road, Mailstop RL 10, Richardson, Texas 75080, United States

Supporting Information

ABSTRACT: Hydrolytically stable, tunable modulus polymer networks are demonstrated to survive harsh alkaline environments and offer promise for use in long-term implantable bioelectronic medicines known as electroceuticals. Today's polymer networks (such as polyimides or polysiloxanes) succeed in providing either stiff or soft substrates for bioelectronics devices; however, the capability to significantly tune the modulus of such materials is lacking. Within the space of materials with easily modified elastic moduli, thiol−ene copolymers are a subset of materials that offer a promising solution to build next generation flexible bioelectronics but have typically been susceptible to hydrolytic degradation chronically. In this inquiry, we demonstrate a materials space capable of tuning the substrate modulus and explore the mechanical behavior of such networks. Furthermore, we fabricate an array of microelectrodes that can withstand accelerated aging environments shown to destroy conventional flexible bioelectronics.

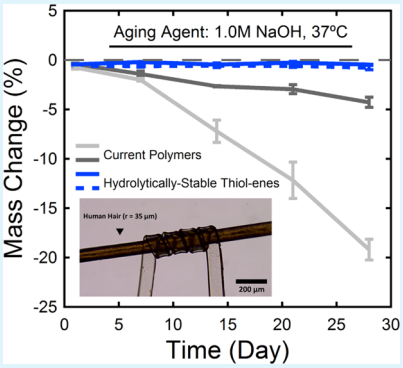

KEYWORDS: *thiol−ene, degradable, tunable modulus, hydrolytic stability, flexible bioelectronics*

1. INTRODUCTION

Current research into the development of therapeutic techniques for disease treatment and prevention has turned to a new class of biomedical technologies: electroceuticals.[1] These electronic devices interface with the body's central and peripheral nervous systems to deliver targeted electrical stimulation to physiologies scaling from a complete nerve, consisting of multiple axons and connective tissue, down to a singular neural cell. Within this paradigm, a variety of devices have been engineered to tackle systemic challenges in the brain,[2−4] spinal cord,[5,6] and viscera.[7,8] However, fundamental engineering challenges remain in enabling a device with chronic performance that can withstand a lifetime of use by the patient and be ultimately compatible with the soft tissues typically surrounding the electroceutical. In this study we evaluate a materials space which enables researchers to produce vitreous, viscoelastic, or elastomeric substrates for use *in vivo,* while investigating the chronic stability of this electroceutical component (the substrate) in the aqueous conditions found *in vivo* through an alkaline accelerated aging environment. Specifically, thiol−ene chemistries are employed for substrate fabrication due to their wide range of tunable chemical and thermomechanical properties,[9] along with previous successful deployments in model electroceuticals.[10]

The suite of thiol−ene chemistries has been demonstrated to provide a versatile toolbox for use in many biomedical applications ranging from the synthesis of drug delivery vehicles[11] to the protection of protein bioactivity.[12] Other macroscale applications have also been developed, including substrates for implantable electronics[10] and flexible thin film organic electronic devices such as mechanically adaptive transistors.[13] Within the space of flexible bioelectronics substrates, the thiol−ene polymerization mechanism provides for a low cure-stress network, which allows for polymer substrates that are compatible with processing via traditional photolithographic techniques.[14] However, in many cases there is an inherent hydrolytic instability of the polymerized network due to the presence of ester linkages in the thiol monomers used for bulk, solvent-free thiol−ene polymerizations. While hydrolytically stable thiol monomers exist, they either form amorphous materials with a low glass transition temperature (aliphatic) or are not readily processable (aromatic) without the use of solvents or elevated temperatures. Instead, many thiol monomers are synthesized through the ester forming, condensation reaction of 3-mercaptoproprionic acid and a multifunctional alcohol.[15,16] While this synthetic route for multifunctional thiol monomers yields products with various types of tunable and desirable properties,[9,17] these monomers all share one common trait: the final monomer is susceptible to hydrolytic degradation back to the original acid and alcohol when exposed to an aqueous environment.[18] Additionally, with the increasing degradation of the ester linkages under aqueous conditions, the formation of acid serves to autocatalyze the reaction, leading to a more rapid and substantial degradation of

Received: November 3, 2015
Accepted: December 9, 2015
Published: December 9, 2015

DOI: 10.1021/acsami.5b10593
ACS Appl. Mater. Interfaces 2015, 7, 28673−28681

the material over time.[19] Due to this hydrolysis, any electronic device fabricated atop hydrolytically sensitive substrates risks catastrophic failure at a chronic time-scale in terms of device performance and ultimate functionality. In demonstrating hydrolytic degradation, Podgórski et al. have recently demonstrated the need for ester-free thiol monomers in systems for chronically viable dental resins using a rigid, low viscosity, hydrolytically stable tetrathiol.[20] While this enables the stability of the network in aqueous media, further control is needed to tune thermomechanical properties for responsive bioelectronics.

In addition to hydrolytic stability, the ability to regulate the modulus when the material is above its glass transition temperature (T_g) enables accommodation of tight bending radii-of-curvature or other severe deformations. A lower rubbery shear modulus (G_r) enabled by decreasing cross-link density allows for further softening of the material as the T_g is surpassed. This phenomenon facilitates not only many biomedical applications requiring low-modulus substrates for chronic interfaces with soft tissues[21] but also compliant substrates for enabling increasingly smaller radii-of-curvature in conformable substrates.[22] Therefore, for flexible bioelectronics, it is important to control the cross-link density of the substrate material to a degree where G_r can be engineered for the specific field of use. However, with a decreased degree of cross-linking there is a corresponding depression of the T_g[23] in addition to the expected decrease in G_r.[24] While other groups have been able to successfully demonstrate low cross-link density thiol−ene materials, the flexible aliphatic linkages exhibit too much steric flexibility such that the polymerized networks rarely exhibit transitions above 0 °C.[25,26] Hence a driving challenge becomes the depression of cross-link density while maintaining a sufficiently rigid polymer backbone to allow for a glass transition above ambient temperatures. By incorporating hydrolytically stable linkages along the backbone of the polymer, a group of thiol−ene materials can be synthesized with the ability to resist degradation in aqueous environments while also softening sufficiently to match the modulus of soft tissues or deploy constrained bioelectronics.

In this work we present a hydrolytically stable thiol−ene system for substrate materials used in flexible bioelectronics, with a specific case study of a microelectrode array that is artificially aged in harsh alkaline environments to mimic chronic hydrolytic degradation. By selecting two aliphatic-core dithiol monomers in conjunction with multifunctional alkene monomers that possess hydrolytically robust backbones, we demonstrate a hydrolytically stable system capable of tuning the T_g between 0 and 80 °C. Further we show that by diminishing our cross-link density through the substitution of a rigid triene with a similarly rigid diene, the ultimate stiffness of the substrate material is similarly tuned into the kPa regime, allowing for the synthesis of vitreous, viscoelastic, or elastomeric compositions at a single reference temperature with minimal chemical distinction between compositions.

2. EXPERIMENTAL SECTION

Commercial Materials and Polymer Synthesis. 1,3,5-Triallyl-1,3,5-triazine-2,4,6(1H,3H,5H)-trione (TA), 2,2′-diallyl bisphenol A diacetate ether (DA), tricyclo[5.2.1.0^{2,6}]decanedimethanol diacrylate (DAc), and 2,2-dimethoxy-2-phenylacetophenone (DMPA) were purchased from Sigma-Aldrich. Trycyclodecane dithiol (DT1) was synthesized with the procedure described in the Supporting Information. 1,10-Decanedithiol (DT2) was purchased from TCI Chemicals. Samples of tris[2-(3-mercaptopropionyloxy)ethyl] isocyanurate (TT) were graciously acquired from Bruno Bock. Sylgard 184 Silicone Elastomer (PDMS) was purchased from Dow Corning. Thiol−ene networks were formed via the stoichiometric balance of reactive functionalities of all comonomers, corrected for the contribution of each monomer's reactive group described in Figure 2. A total of 1 wt % DMPA of total monomer weight was dissolved in the solution for the initiation of the photopolymerization of the monomer solution. The resin was then encased between glass slides spaced by a 1 mm thick glass shim. Thiol−ene/acrylate networks were fabricated in a similar method utilizing only 0.1 wt % DMPA of total monomer weight. All thiol−ene networks were cured in a 365 nm UV retrofitted Thermo Scientific oven at 100 °C for 2 h. Cured samples were then placed in a vacuum oven at 120 °C, 5inHg for 24 h to further complete network conversion. Cross-linked PDMS samples were prepared via a 1:10 addition of curing agent to prepolymer and a thermal cure at 60 °C for 1 h.

Dynamic Mechanical Analysis. Dynamic mechanical analysis (DMA) was performed on a Mettler Toledo DMA 861e/SDTA. Samples were cut into cylinders approximately 1 mm thick and ∼3 mm in diameter. The mode of deformation was shear and strain was limited to a maximum of 0.3%. Samples were tested at a heating rate of 2 °C min^{-1}. The frequency of deformation shown is 1 Hz. Tests were conducted in a nitrogen atmosphere. Each composition was tested at least twice. All modulus data presented here is the shear modulus. The shear modulus (G) is related to the Young's modulus (E) through Poisson's ratio (ν) as given by $G = E/2(1 + \nu)$. Poisson's ratio was not measured for these polymers; however, ν can be generally taken as approximately 0.35 for glassy polymers and 0.5 for polymers above the glass transition.

Tensile Testing. Tensile testing results were gathered using an Instron Model 5848 Microtester. Samples were cast according to the previously described methodology as 125 μm sheets. Next, films were laser micromachined into dogbones 37.3 mm long and 1 mm wide in the gage region. Data was recorded using a 50 N load cell and a crosshead extension speed of 5 mm min^{-1}.

Scanning Electron Microscopy. Scanning electron microscopy was performed in a ZEISS SUPRA-40. Samples were sputtered with gold to reduce the charging effect. Images were captured at a working distance and electron high tension of 25 mm and 5 keV, respectively.

Swelling and Mass Loss Measurements. Swollen weight was measured by weight change after immersion in one molar sodium hydroxide (1.0 M NaOH) solution at 37 °C at four time points over 1 month. Samples consisted of ∼10 mg mechanically excised cylinders 3 mm in diameter and 1.2 mm in height. The dry mass of each sample was measured and recorded with an ultramicrobalance with 0.1 μg precision. At each desired time point, each sample was removed from the solution, and the surface of the polymer was gently dried using an absorbent wipe. The swollen mass was then recorded. Mass loss was measured after samples were placed atop a polytetrafluoroethylene (PTFE) block inside of a vacuum oven at 120 °C, 5 inHg for 24 h. The samples were then removed and reweighed for the final mass lost. Swelling is calculated as the mass percent change from swollen mass to vacuum oven-dried mass. Mass loss is calculated as the mass percent change from initial weight to vacuum oven-dried mass. Data reported are the average of four samples.

Device Aging and Imaging. Devices were immersed in a sealed container (Teflon PTFE threaded cap) with 10 mL 1.0 M NaOH. At each time point, devices were carefully removed and thoroughly rinsed with deionized water (diH_2O). Afterward, the devices were laid atop a cleaned glass slide and heated to at least 80 °C to soften each device and conform the substrate to the planar slide. The slide was then imaged using a Leica DM4000 M LED upright microscope using a 10X objective lens.

Device Substrate Preparation. 75 × 50 mm glass microscope slides were cleaned by subsequent steps of scrubbing in an Alconox solution, sonication in acetone, and sonication in isopropyl alcohol and repeated as necessary until free of optically visible unwanted material. 300 nm of Au was deposited at 0.2 nm s^{-1} using electron-beam evaporation. Metal transfer was accomplished by using a sacrificial

DOI: 10.1021/acsami.5b10593
ACS Appl. Mater. Interfaces 2015, 7, 28673−28681

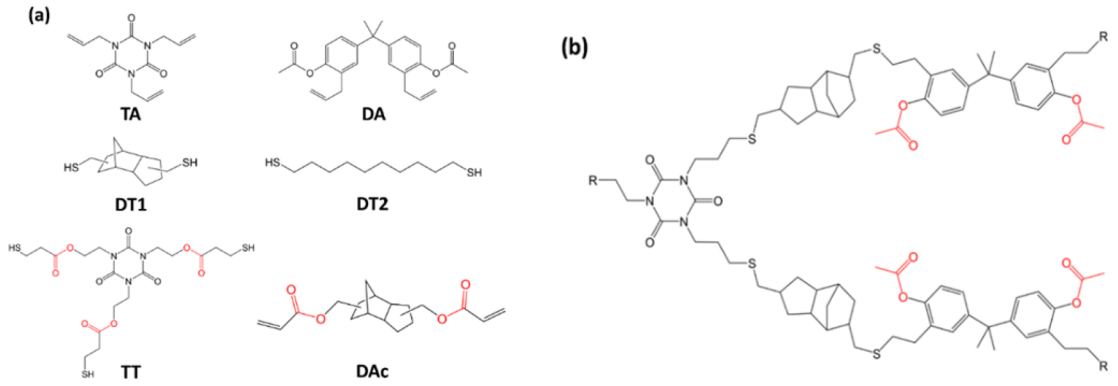

Figure 1. Summary of (a) monomers used in hydrolytically stable thiol−ene compositions and (b) example network backbone containing no hydrolytically sensitive groups (shown in red) on the backbone.

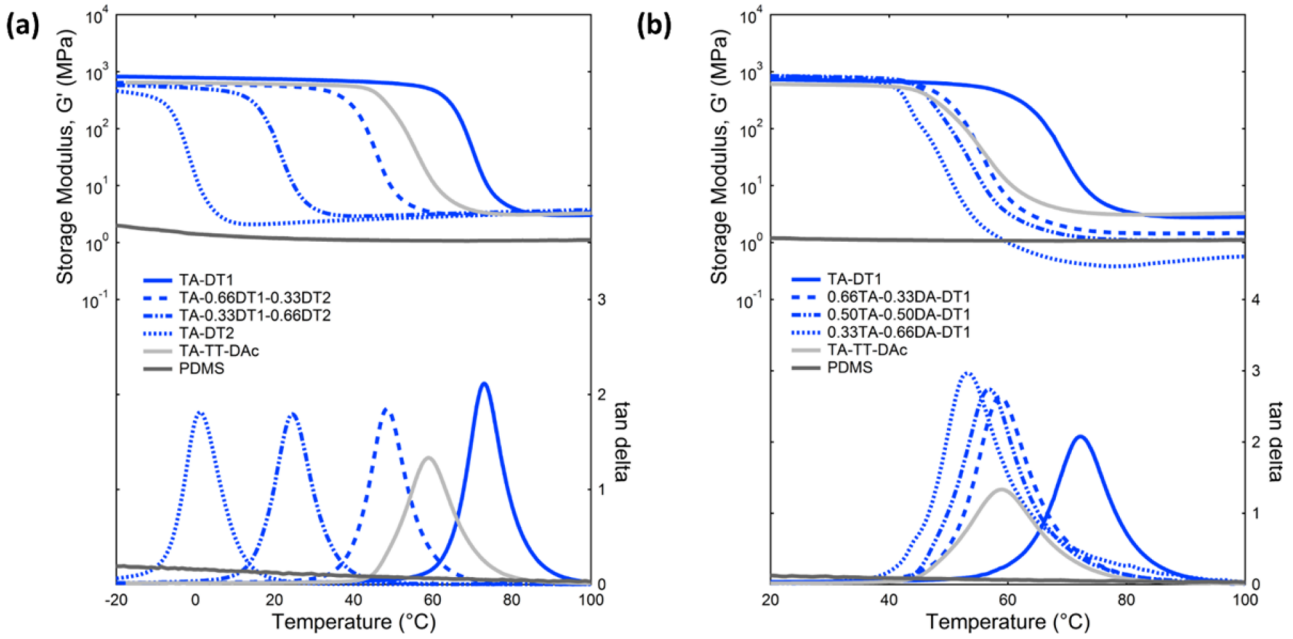

Figure 2. Dynamic mechanical analysis (DMA) shows shear storage modulus G' and glass transition temperature (T_g) as measured by the peak in the damping factor (tan delta) of hydrolytically stable thiol−ene networks for (a) thiol tuned materials from −20 to 100 °C and (b) alkene tuned compositions from +20 to 100 °C in comparison to hydrolytically active thiol−ene/acrylate and polydimethylsiloxane networks.

glass substrate with an unpatterned gold film as the bottom slide for the mold with the metal surface facing inward. The top side of the mold was a cleaned glass slide.

Metal Patterning. Electrodes were then patterned by standard photolithography using S1813 photoresist (Microposit). Briefly, the resist was spun onto the metal coated polymer at 2000 rpm with an acceleration of 3000 rpm s^{-1}. The resist was then soft-baked at 85 °C for 10 min. A pattern was transferred to the resist using UV light at a dose of 150 mJ cm^{-2}. The resist was developed using MF-319 Developer and subsequently hard-baked at 85 °C for 10 min. Metal was then etched using gold etchant (AU-5 Cyantek Corporation).

Parylene-C Deposition and Patterning. 500 nm of Parylene-C was deposited using a Labcoater 2 (SCS Systems). Patterning of the photoresist was accomplished through similar methods described during metal patterning. Parylene-C was etched using a Technics reactive ion etching tool using oxygen plasma. A pressure of 140 mTorr and power of 50 W were used. Each sample was etched for 8 min. After RIE the photoresist was removed using a flood exposure and subsequent developing.

Device Definition. Micromachining was performed using a frequency tripled YAG laser connected to a μFab workstation (Newport). Devices were removed from the carrier glass slide by lifting gently with a moistened razor blade.

3. RESULTS

Monomers were chosen for this study based on the hydrolytic insensitivity of the molecular backbone connecting the reactive moieties (Figure 1a). The trifunctional alkene, 1,3,5-triallyl-1,3,5-triazine-2,4,6-(1*H*,3*H*,5*H*)-trione (TA), and difunctional alkene, 2,2′-diallylbisphenol A diacetate ether (DA), were chosen based on their relative monomer backbone rigidity while maintaining the ability to modulate the cross-link density. While the dithiol, tricyclodecane dithiol (DT1), has been reported before in patent literature,[27] its academic use has not previously been discussed to the authors' knowledge. The synthetic procedure for producing this dithiol can be found in the Supporting Information along with NMR spectra of the final product (Figures S6 and S7). Due to the rigid tricyclodecane core connecting the two thiol functionalities, this molecule imparts a stiffer dithiol connection between the alkene monomers and raises the temperature required for

DOI: 10.1021/acsami.5b10593
ACS Appl. Mater. Interfaces 2015, 7, 28673−28681

polymer segment motion. In stark contrast, the dithiol 1,10-decanedithiol (DT2) was chosen for its greater flexibility in comparison to DT1 while maintaining a similar molecular weight. Hydrolytically sensitive monomers containing hydrolyzable ester linkages include the diacrylate tricyclo[5.2.1.0^{2,6}]-decanedimethanol diacrylate (DAc) and the trifunctional thiol tris[2-(3-mercaptopropionyloxy)ethyl] isocyanurate (TT), used in the synthesis of the hydrolytically sensitive thiol−ene neural interface substrate. Using the hydrolytically stable monomers (top four from Figure 1a), a variety of thiol−ene networks were formed that showed hydrolytic stability along the backbone of the final cross-linked network (Figure 1b).

Dynamic mechanical analysis (DMA) was performed on networks to demonstrate both precise control over the glass transition temperature, as defined by the peak of tan delta, and a tunable rubbery shear modulus. Two other materials found extensively in the literature were also explored for mechanical properties and hydrolytic inertness: the commonly used silicone elastomer, polydimethylsiloxane (PDMS - Sylgard 184, 10:1 prepolymer to curing agent ratio), and a previously described thiol−ene/acrylate system (TA-TT-DAc).[28] Using the trifunctional monomer TA as a constant, the dithiol concentration was varied from flexible (TA-DT2) to rigid (TA-DT1) with two other intermediate networks. As seen in Figure 2a, the TA-based networks demonstrated a T_g range spanning almost 80 °C solely by tuning the molar concentration of DT1 to DT2 while maintaining the same modulus below and above their respective transition temperatures. The G_r of the material was also modulated by reducing the average functionality of the monomers. By substituting an increasing amount of the alkene functionality due to TA with the moiety contribution from DA, a higher molecular weight between cross-links was observed via the reduction of G_r in subsequent compositions (Figure 2b).

All thermomechanical data from the explored networks were tabulated and condensed to four polymers of interest in Table 1. The DT1-containing network with the highest glass transition temperature and the lowest rubbery modulus (TA-DT1 and 0.33TA-0.66DA-DT1, respectively) was chosen from all of the new networks explored in Figure 2. Additionally, the previously described thiol−ene/acrylate system (TA-TT-DAc) was selected alongside the commonly used elastomer PDMS. Thermomechanical characterization, such as the T_g (recorded as the peak of the tangent delta curve) and the breadth of the transition (measured as the full-width half max [fwhm] of the tangent delta curve), is shown for the three thiol−ene(acrylate) networks showing a relatively homogeneous network distribution with very sharp transition temperatures as denoted by the near single-digit fwhms. Similar data for the PDMS network was not within the range of measurements capable of using the instrumentation employed in this study, however, a literature precedent from Clarson et al. gives insights into the low transition temperature of the silicone elastomer (T_g = −125 °C).[29] All rubbery modulus values were recorded at T_g + 25 °C (except in the case of the PDMS elastomer where the G_r was recorded at 80 °C) such that the ultimate cross-link density of the polymer could be analyzed in accordance with eq 1

$$\nu = \frac{G_r}{RT} \tag{1}$$

where ν is the cross-link density measured in moles per liter or molarity (M), G_r is the shear elastic modulus (MPa), R is the ideal gas constant (L MPa K^{-1} mol^{-1}), and T is the absolute temperature at which the shear elastic modulus was measured (K). Of note is the cross-link density of the 0.33TA-0.66DA-DT1 system, which shows the lowest cross-link density average of 0.14 M, lower than the PDMS elastomer studied herein which is typically used for its low modulus properties in flexible electronics.[6,30] To quantify the effects of varying the molar ratios of the rigid versus flexible dithiols and the trifunctional versus difunctional alkene on the glass transition temperature, the T_g (as denoted by the peak of tan delta in DMA) of hydrolytically stable networks was graphed against the molar ratio of DT1 (Figure S9a) and the molar ratio of DA (Figure S9b). A linear regression analysis of the transition temperature versus molar ratios of DT1 reveals a highly correlated response in increasing T_g with increasing molar ratio of DT1 (r^2 > 0.99) and decreasing T_g with increasing molar ratio of DA (r^2 = 0.95), indicating a highly linear response between modifying monomer molar content and the resultant T_g.

Using the monomer space defined in Figure 2, example networks with low cross-link density were fabricated to demonstrate a vitreous (T_g = 50 °C), viscoelastic (T_g = 25 °C), and elastomeric (T_g = 0 °C) composition at the same ambient temperature of 25 °C. Figure 3 demonstrates the tensile testing results of these compositions along with the average failure stress, failure strain, and toughness across four samples of each material. While the vitreous composition demonstrates the highest tensile strength of 11.3 MPa, the samples are brittle and exhibit failure at only 0.7% strain. Conversely, the elastomeric sample reaches only 15% of the yield strength seen in the vitreous material but can accommodate an average strain of 141% while demonstrating a network that is over 20 times tougher than the vitreous network. The viscoelastic composition is the toughest composition with a mean toughness value of 4.90 MJ m^{-3} with intermediate failure stresses and failure strains measured (5.90 MPa and 119%, respectively) as compared to the vitreous and elastomeric networks.

By next using the substrate with a combination of the highest T_g and lowest G_r (0.33TA-0.66DA-DT1), preliminary conformability of the substrate was explored in a helical formation of the material around a 70 μm thick human hair. The optical micrograph of the helix configuration (Figure 4a) shows a tight radius-of-curvature vitreous material that was curved around a human hair while heated above the T_g and then cooled to an ambient temperature where the material maintained the helical shape around the hair strand without fracture of the 35 μm-thick substrate. As the human hair can be clearly seen through the material in Figure 4a, preliminary optical properties were measured using UV−vis spectroscopy (Figure S10) showing the decreased transparency of the 0.33TT-0.66DA-DT1

Table 1. Thermomechanical Characterization of the Four Networks Studied for Advanced Hydrolytic Resistance, Including the T_g by DMA (Peak of Tan Delta), the Full-Width Half Max (fwhm) of the Glass Transition, and the Rubbery Modulus at 25 °C above the T_g with the Corresponding Cross-Link Density (ν) Calculation; n = 3

network	T_g (°C)	fwhm (°C)	G_r (MPa)	ν (M)
TA-DT1	72.5 ± 0.3	10.9 ± 0.2	2.77 ± 0.26	0.90 ± 0.08
0.33TA-0.66DA-DT1	54.1 ± 1.3	11.3 ± 1.2	0.41 ± 0.04	0.14 ± 0.01
TA-TT-DAc	59.9 ± 1.7	16.3 ± 2.1	3.55 ± 0.40	1.19 ± 0.13
PDMS	−125*		1.12 ± 0.04	0.38 ± 0.01

DOI: 10.1021/acsami.5b10593
ACS Appl. Mater. Interfaces 2015, 7, 28673−28681

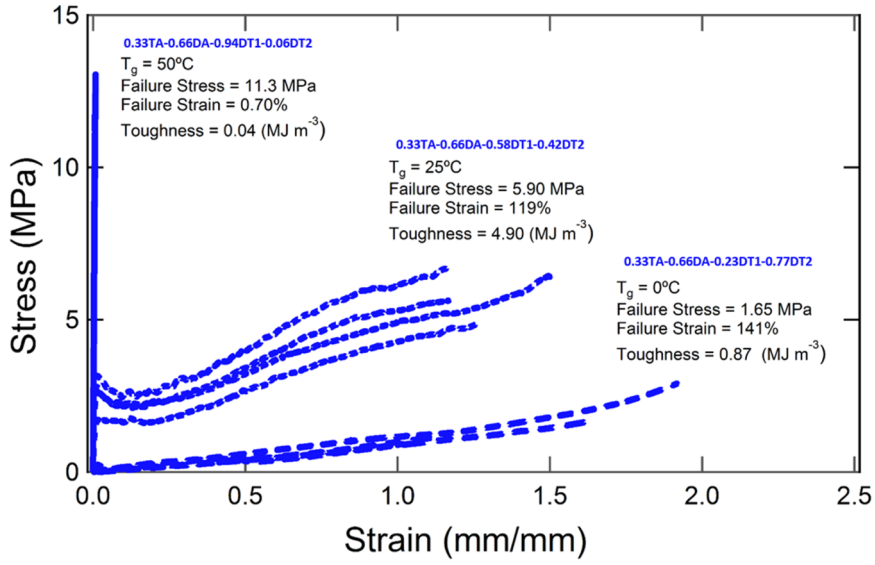

Figure 3. Tensile testing results of DT1-DT2/TA-DA formulations designed for glassy, viscoelastic, or elastomeric behavior at room temperature (25 °C), along with summary statistics on failure stress, failure strain, and toughness (n = 4, standard deviations shown in text).

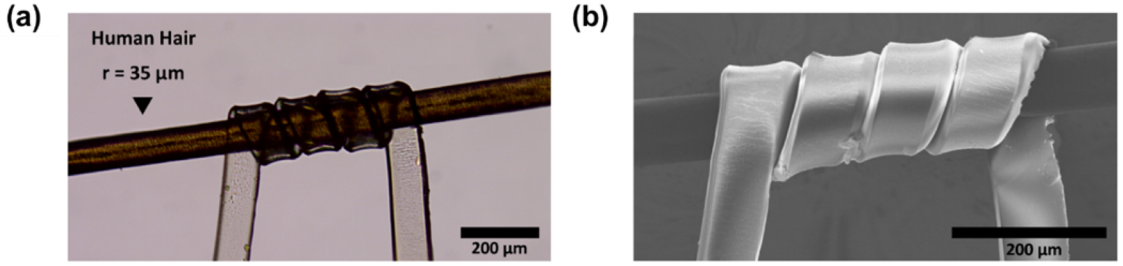

Figure 4. Optical (a) and scanning electron (b) micrographs of tight radius-of-curvature (<50 μm) polymer helices enabled by the softening composition 0.33TA-0.66DA-DT1 allow for interface with small structures such as a 35 μm radius human hair.

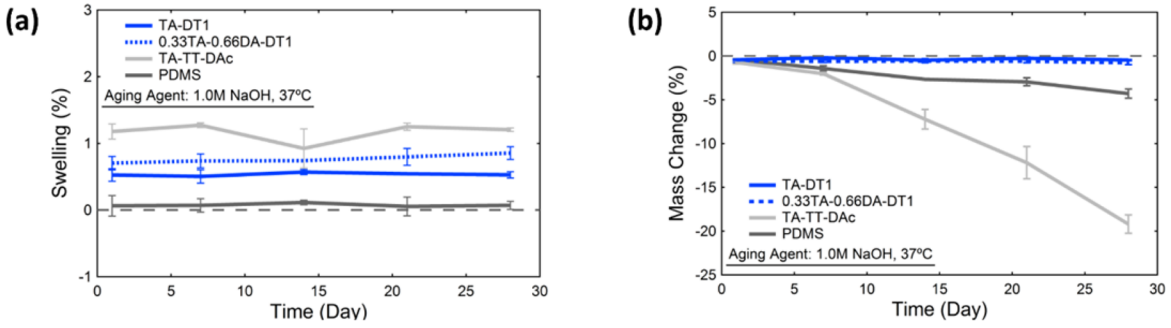

Figure 5. (a) Swelling characteristics of substrates for flexible bioelectronics with (b) corresponding mass loss curves.

material relative to the hydrolytically sensitive TT-TA-DAc network. Next, in Figure 4b we observe the scanning electron micrograph of this same helix showing the curvature enabled by a softening substrate which is easily handled at room temperature (below the T_g) yet conforms to three-dimensional targets with a radius-of-curvature less than 50 μm. The temporary helical shape was maintained around the human hair without external load, showing promise for using this materials space as shape memory materials for flexible bioelectronics such as the 3D conformable cuff electrodes fabricated by Ware et al.[28] With the strain-tolerance demonstrated by the decreased cross-link density networks, future work may also focus on investigating the high strain shape memory properties as previously studied by Voit et al.[31] and Zheng et al.[32]

The hydrolytic sensitivity of the materials was explored in an accelerated aging environment (1.0 M NaOH, 37 °C) in comparison to the other previously described substrates for flexible bioelectronics. Figure 5a shows the swelling behavior of two chosen DT1-based compositions (the highest T_g TA-DT1 material and the lowest cross-link density 0.33TA-0.66DA-DT1 material) versus the control substrates PDMS and TA-TT-DAc. Over the course of the four week observation, no appreciable swelling of the hydrophobic PDMS substrate was observed. The thiol−ene/acrylate composition TA-TT-DAc demonstrated the highest swelling ratio with roughly 1.2% fluid uptake across the month-long period. Finally, the DT1 containing

DOI: 10.1021/acsami.5b10593
ACS Appl. Mater. Interfaces 2015, 7, 28673−28681

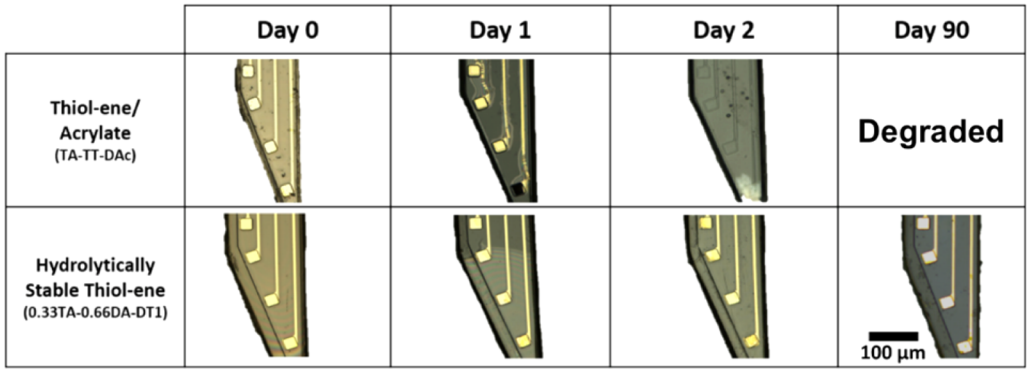

Figure 6. Optical micrographs of example neural electrodes as fabricated on hydrolytically sensitive and stable thiol−ene based networks over 90 days in 1.0 M NaOH at 37 °C.

compositions showed an intermediate swelling with an almost constant 0.5% swollen content in the TA containing network and 0.7% in the 0.33TA-0.66DA network. While there was a slight increase in the average swelling from 0.7% to 0.85% in the 0.33TA-0.66DA material, no statistical significance was observed for this change. This minor increase in swelling percentage in the 0.33TA-0.66DA-DT1 network could indicate an increased hydrophilicity of the network over time, representative of the inherent increase in hydrophilicity due to the acetate moieties on the bisphenol A core, as well as a possible evolution of hydroxyl side groups as the acetate groups are hydrolytically cleaved *in vitro*. When looking at mass change with respect to the initial dry mass of the network in Figure 5b, both DT1 compositions were observed to have no appreciable mass loss during the month-long study. The PDMS and TA-TT-DAc networks however had demonstrated significant mass loss by day 28, with roughly 5% mass loss in the PDMS network and 20% mass loss in the TA-TT-DAc network. For ester containing networks such as the TA-TT-DAc polymer, this degradation profile shows a similar degradation *in vitro* as a recently published study by Podgórski et al. which used comparable accelerated aging conditions (0.1 M NaOH).[20] The hydrolytic activity *in vitro* suggests a sensitivity of these substrates to aqueous environments where main chain degradation and solvation of the degradable components lead to an unstable substrate for chronically viable flexible bioelectronics exposed to wet conditions. Independent of the swelling ratio, degradation of polymer networks is directly related to the presence of hydrolyzable linkages in the backbone of the substrate material. Thus, the PDMS (siloxane-linked) and TA-TT-DAc (ester-linked) networks degrade, while the TA-DT1 and 0.33TA-0.66DA-DT1 materials do not degrade.

Finally the hydrolytic stability of substrates explored in this study was highlighted in Figure 6 where a set of flexible electrodes, similar to devices which have been previously used as intracortical interfaces,[10] was fabricated atop two separate thiol−ene based substrates, the hydrolytically sensitive TA-TT-DAc and the hydrolytically stable 0.33TA-0.66DA-DT1. After devices were fabricated atop both substrates, they were immersed in the same aging agent used for swelling and mass loss, 1.0 M NaOH at 37 °C. At Day 0, both substrates were pristine, and the microfabricated electronics were fully encapsulated. By Day 1, the hydrolytically sensitive substrate already began demonstrating warping of the encapsulation and slight delamination of the passive electronics, whereas the 0.33TA-0.66DA-DT1 substrate showed no such defects. On Day 2 there was a full loss of the device fabricated atop the TA-TT-DAc substrate, whereas again no change was noticed in the hydrolytically stable thiol−ene based probes. For the sake of demonstrating substrate longevity and not solely acute resistance, the substrates were sealed in the aging agent and reimaged after 90 days to see the long-term effect on the substrate. The hydrolytically sensitive TA-TT-DAc substrate had by this point completely degraded, leaving a free-floating bilayer of the encapsulation and conductive traces. However, in the hydrolytically stable compositions virtually no morphological change was observed even after three months of immersion in the harsh alkaline environment.

4. DISCUSSION

The fundamental goal of this study is the realization of a thiol−ene materials system which presents a flexibility in designing vitreous, viscoelastic, or elastomeric polymer substrates for flexible bioelectronics. With much of the electroceutical community focused on the design of novel devices on traditional substrates such as polyimides[33,34] and polysiloxanes,[6,35] this work aims to innovate on the networks used beneath the passive and active components integrated atop flexible substrates. Specifically using a liquid four-monomer system, vitreous, viscoelastic, and elastomeric compositions are demonstrated and mechanically tested at the same ambient temperature. In addition to the desirable mechanical property space explored herein, the materials are also evaluated for long-term compatibility in aggressive alkaline solutions, simulating a chronic usage in the aqueous *in vivo* environments to which they are expected to be exposed.

While commercially available monomers can be chosen for this materials system, the increase in difficulty of processing (such as excessive heat or the use of solvents) attributed to the introduction of crystalline polythiols necessitates a new rigid dithiol for use as an inflexible chain-extender during the fabrication of high-T_g substrates. For this goal a new molecule is synthesized, referred to in this study as tricyclodecane dithiol or DT1 (Figure 1a), and incorporated into a wide range of polymer networks using the thiol-click polymerization mechanism. The resultant thermomechanical properties of the network are investigated and analyzed to ensure a precise control over the modulation of the T_g and G_r. For these networks, Figure 2 shows a summary of the thermomechanical data from the thiol−ene systems using the new molecule DT1 in conjunction with other commercially available substrates. Using this four-component monomer solution, a range of

DOI: 10.1021/acsami.5b10593
ACS Appl. Mater. Interfaces 2015, 7, 28673−28681

tunable glass transition temperatures is shown from 0 to 80 °C (Figure 2a), and the ability to depress the rubbery shear modulus of the material to as low as 600 kPa in shear is also demonstrated (Figure 2b). This summary data is compared to a previously studied thiol−ene material[10] and a commonly used elastomer (the polydimethylsiloxane Sylgard 184, 10:1 prepolymer to curing agent ratio) in order to show the tunable nature of the elastic modulus in this materials space. Preliminary trend line fitting indicates that there is a linear correlation (Figure S9a) between the expected T_g and the molar ratios used of DT1 when the alkene comonomer molar ratios are maintained constant. This phenomena allows for the prediction of transition temperature and therefore modulus at a specific temperature before experimentation. Similarly in accordance to the theory proposed by Nielsen, the depression of cross-link density (and therefore the G_r) via the increase of DA molar content is also explored and shows a corresponding decrease in the glass transition temperature (Figure S9b).[24] Normally, this low cross-link density results in a thiol−ene material with a subambient glass transition temperature that removes the possibility of the material's use in carrier-free, implantable bioelectronics such as the microelectrode arrays fabricated in this work. However, due to the molecular rigidity of the intrathiol linkage in the molecule DT1, a similar T_g is observed in the 0.33TA-0.66DA-DT1 network as the TA-TT-DAc network, despite over an order of magnitude depression in the cross-link density (Table 1).

More relevant to isothermal uses such as implantable bioelectronics which are maintained at a relatively constant temperature of 37 °C, the materials space can be utilized to show vitreous, viscoelastic, or elastomeric behavior through the tuning of the component molar ratios as shown in Figure 3. While this demonstration shows a reference isothermal test at 25 °C due to the lack of an environmental chamber surrounding the tensile testing unit, the varied modulus and failure parameters of the three compositions explored exhibit that a number of substrates can be imagined with minimal chemical makeup differentiation but with significantly different stress- and strain-tolerances. Of note is the vitreous composition shown in Figure 3, which demonstrates a significantly lower yield strength than many other glassy polymers used for flexible electronics such as polyimide or Parylene.[34,36] While these materials may present more successful vitreous alternatives to the materials in this study, the challenge becomes rapidly modulating the modulus of the substrate based on device need. For applications requiring interfaces with soft tissues such as the brain, this materials space provides a facile toolbox in creating substrates capable of chronic stiffness, as well as softening archetypes.

For vitreous samples with the lowered cross-link density of the 0.33TA-0.66DA-DT1 network, such a material not only enables apparent softening at elevated temperatures above the transition temperature but also presents the possibility for interacting with complex three-dimensional geometries at new scales. Figure 4 explores such a use in a helical design where the low-modulus of the material in the rubbery state allows for tight conformability to a substrate with a radius-of-curvature less than 50 μm, such as the human hair pictured. By elevating the temperature above the T_g of the pictured material, the elastomeric nature of the film at the new temperature allows for intimate interfacing between the surface of the polymer and the hair strand. Importantly, the material can then be cooled to ambient temperature and retain its helical shape with no external loading, therefore maintaining the intimate contact with a target microstructure such as a hair or a nerve without flexural stress imposed on the structure from having to maintain the elastomeric substrate in tension against the target.

In addition to evaluating the mechanical properties of the materials designed in this study, the hydrolytic stability is studied in these networks by reducing or completely eliminating hydrolytically labile sites such as those highlighted red in Figure 1b. These sites present a point of failure for the material in aqueous conditions as either slightly acidic or basic conditions can catalyze breakdown of these linkages and lead to material degradation.[20] With the DT1 molecule and the other hydrolytically inactive commercial monomers chosen in this study, the networks fabricated were explored and validated in harsh aqueous environments. Figure 5 shows the swelling and mass loss characteristics of a select few DT1-containing networks against the two hydrolytically unstable networks chosen as controls: PDMS and TA-TT-DAc. While the swelling curves show little variation in the fluid uptake of the network week-to-week, the degradation curves (Figure 5b) show the principle point of adding DT1 to the polymer networks: DT1-containing polymers exhibited no appreciable degradation over a month-long immersion in 1.0 M NaOH. This observation suggests a strong resistance to base-catalyzed hydrolytic stability that, given Podgórski's earlier report, indicates a hydrolytic stability in the acid-catalyzed case as well.[20]

To test this stability in a more relevant system for flexible electronics, the bare polymer must be incorporated into an electronic device which can demonstrate hydrolytic stability. This is most clearly shown in Figure 6, where a set of example bioelectronic devices is fabricated on both the hydrolytically stable 0.33TA-0.66DA-DT1 network as well as the hydrolytically susceptible TA-TT-DAc network, in accordance with the photolithographic procedures previously outlined.[4] The representative devices are then immersed in a 1.0 M NaOH solution at 37 °C and imaged every 24 h to observe any morphological changes. While the imaging shows that the hydrolytically sensitive thiol−ene/acrylate systems were degraded within a few days of suspension in 1.0 M NaOH, the DT1-containing network showed virtually no morphological changes even up to a three-month immersion. This optical evidence does not speak to the electrical performance of the devices atop either substrate, as issues with encapsulation and interfacial fluid buildup can still hinder device performance. However, the ability of the substrate to withstand aggressive aqueous conditions shown in this work allows for more interesting and long-term device fabrication strategies for electroceutical therapies.

5. CONCLUSION

In this work we demonstrate a tunable modulus, hydrolytically stable thiol−ene framework for substrates utilized in electroceuticals, with a targeted focus on biomedical implants immersed in aqueous environments such as neural prosthetics. Through the use of the rigid aliphatic dithiol DT1, networks with high softening temperatures (up to 80 °C) are synthesized and show not only a precise ability to tune the transition temperature but also the cross-link density utilizing only a four component system. These networks exhibit no appreciable mass change in harsh hydrolytic conditions, in stark contrast to other lab scale and commercially available substrates for flexible bioelectronic devices. Future work will focus primarily on engineering the network for plasticization *in vitro* and *in vivo* to

DOI: 10.1021/acsami.5b10593
ACS Appl. Mater. Interfaces 2015, 7, 28673−28681

allow for a similar acutely stiff but chronically soft archetype seen previously in the neural interface literature,[2,10] as well as active electronics requiring softening, flexible substrates.[13]

■ ASSOCIATED CONTENT

Supporting Information

The Supporting Information is available free of charge on the ACS Publications website at DOI: 10.1021/acsami.5b10593.

Synthetic procedure for DT1 monomer in Figure 1; Figures S1−S8, characterization of DT1 monomer and the intermediate products; Figure S9, glass transition temperature dependence of networks formed as a function of the (a) DT1 concentration and (b) DA concentration; and Figure S10, UV−vis spectra for the TA-TT-DAc and 0.33TA-0.66DA-DT1 networks (PDF)

■ AUTHOR INFORMATION

Corresponding Author

*E-mail: taylor.ware@utdallas.edu.

Author Contributions

The manuscript was written through contributions of all authors. All authors have given approval to the final version of the manuscript.

Notes

The authors declare no competing financial interest.

■ ACKNOWLEDGMENTS

The authors would like to thank the National Science Foundation Graduate Research Fellowship Award No. DGE-1147385, Margaret McDermott and the Eugene McDermott Graduate Fellows Program, and the Defense Advanced Research Projects Agency (DARPA)/MTO Young Faculty Award (YFA) Grant No. D13AP00049.

■ REFERENCES

(1) Famm, K.; Litt, B.; Tracey, K. J.; Boyden, E. S.; Slaoui, M. Drug Discovery: A Jump-Start for Electroceuticals. *Nature* **2013**, *496*, 159−161.

(2) Harris, J.; Hess, A. E.; Rowan, S. J.; Weder, C.; Zorman, C.; Tyler, D.; Capadona, J. R. In Vivo Deployment of Mechanically Adaptive Nanocomposites for Intracortical Microelectrodes. *J. Neural Eng.* **2011**, *8*, 046010.

(3) Mandal, H. S.; Knaack, G. L.; Charkhkar, H.; McHail, D. G.; Kastee, J. S.; Dumas, T. C.; Peixoto, N.; Rubinson, J. F.; Pancrazio, J. J. Improving the Performance of Poly(3,4-Ethylenedioxythiophene) for Brain−Machine Interface Applications. *Acta Biomater.* **2014**, *10*, 2446−2454.

(4) Ware, T.; Simon, D.; Arreaga-Salas, D. E.; Reeder, J.; Rennaker, R.; Keefer, E. W.; Voit, W. Fabrication of Responsive, Softening Neural Interfaces. *Adv. Funct. Mater.* **2012**, *22*, 3470−3479.

(5) Brus-Ramer, M.; Carmel, J. B.; Chakrabarty, S.; Martin, J. H. Electrical Stimulation of Spared Corticospinal Axons Augments Connections with Ipsilateral Spinal Motor Circuits after Injury. *J. Neurosci.* **2007**, *27*, 13793−13801.

(6) Minev, I. R.; Musienko, P.; Hirsch, A.; Barraud, Q.; Wenger, N.; Moraud, E. M.; Gandar, J.; Capogrosso, M.; Milekovic, T.; Asboth, L.; Torres, R. F.; Vachicouras, N.; Liu, Q.; Pavlova, N.; Duis, S.; Larmagnac, A.; Vörös, J.; Micera, S.; Suo, Z.; Courtine, G.; Lacour, S. P. Electronic Dura Mater for Long-Term Multimodal Neural Interfaces. *Science* **2015**, *347*, 159−163.

(7) Banerjee, S.; Pasricha, P. J. Embracing New Technology in the Gastroenterology Practice. *Clin. Gastroenterol. Hepatol.* **2010**, *8*, 848−850.

(8) Snellings, A. E.; Grill, W. M. Effects of Stimulation Site and Stimulation Parameters on Bladder Inhibition by Electrical Nerve Stimulation. *BJU Int.* **2012**, *110*, 136−143.

(9) Hoyle, C. E.; Lowe, A. B.; Bowman, C. N. Thiol-Click Chemistry: A Multifaceted Toolbox for Small Molecule and Polymer Synthesis. *Chem. Soc. Rev.* **2010**, *39*, 1355−1387.

(10) Ware, T.; Simon, D.; Liu, C.; Musa, T.; Vasudevan, S.; Sloan, A.; Keefer, E. W.; Rennaker, R. L.; Voit, W. Thiol-Ene/Acrylate Substrates for Softening Intracortical Electrodes. *J. Biomed. Mater. Res., Part B* **2014**, *102*, 1−11.

(11) Kim, E.; Kim, D.; Jung, H.; Lee, J.; Paul, S.; Selvapalam, N.; Yang, Y.; Lim, N.; Park, C. G.; Kim, K. Facile, Template-Free Synthesis of Stimuli-Responsive Polymer Nanocapsules for Targeted Drug Delivery. *Angew. Chem.* **2010**, *122*, 4507−4510.

(12) McCall, J. D.; Anseth, K. S. Thiol−Ene Photopolymerizations Provide a Facile Method to Encapsulate Proteins and Maintain Their Bioactivity. *Biomacromolecules* **2012**, *13*, 2410−2417.

(13) Reeder, J.; Kaltenbrunner, M.; Ware, T.; Arreaga-Salas, D.; Avendano-Bolivar, A.; Yokota, T.; Inoue, Y.; Sekino, M.; Voit, W.; Sekitani, T.; Someya, T. Mechanically Adaptive Organic Transistors for Implantable Electronics. *Adv. Mater.* **2014**, *26*, 4967−4973.

(14) Simon, D.; Ware, T.; Marcotte, R.; Lund, B. R.; Smith, D. W., Jr; Di Prima, M.; Rennaker, R. L.; Voit, W. A Comparison of Polymer Substrates for Photolithographic Processing of Flexible Bioelectronics. *Biomed. Microdevices* **2013**, *15*, 925−939.

(15) Roberts, J. S. In *Kirk-Othmer Encyclopedia of Chemical Technology*; John Wiley & Sons, Inc.: 2000.

(16) Roy, K.-M. In *Ullmann's Encyclopedia of Industrial Chemistry*; Wiley-VCH Verlag GmbH & Co. KGaA: 2000.

(17) Lowe, A. B. Thiol-Ene "Click" Reactions and Recent Applications in Polymer and Materials Synthesis. *Polym. Chem.* **2010**, *1*, 17−36.

(18) Uhrich, K. E.; Cannizzaro, S. M.; Langer, R. S.; Shakesheff, K. M. Polymeric Systems for Controlled Drug Release. *Chem. Rev.* **1999**, *99*, 3181−3198.

(19) Siparsky, G. L.; Voorhees, K. J.; Miao, F. Hydrolysis of Polylactic Acid (Pla) and Polycaprolactone (Pcl) in Aqueous Acetonitrile Solutions: Autocatalysis. *J. Polym. Environ.* **1998**, *6*, 31−41.

(20) Podgórski, M.; Becka, E.; Chatani, S.; Claudino, M.; Bowman, C. N. Ester-Free Thiol-X Resins: New Materials with Enhanced Mechanical Behavior and Solvent Resistance. *Polym. Chem.* **2015**, *6*, 2234.

(21) Subbaroyan, J.; Martin, D. C.; Kipke, D. R. A Finite-Element Model of the Mechanical Effects of Implantable Microelectrodes in the Cerebral Cortex. *J. Neural Eng.* **2005**, *2*, 103.

(22) Suo, Z.; Ma, E.; Gleskova, H.; Wagner, S. Mechanics of Rollable and Foldable Film-on-Foil Electronics. *Appl. Phys. Lett.* **1999**, *74*, 1177−1179.

(23) Landel, R. F.; Nielsen, L. E. *Mechanical Properties of Polymers and Composites*; CRC Press: 1993.

(24) Nielsen, L. E. Cross-Linking−Effect on Physical Properties of Polymers. *J. Macromol. Sci., Polym. Rev.* **1969**, *3*, 69−103.

(25) Chan, J. W.; Shin, J.; Hoyle, C. E.; Bowman, C. N.; Lowe, A. B. Synthesis, Thiol− Yne "Click" Photopolymerization, and Physical Properties of Networks Derived from Novel Multifunctional Alkynes. *Macromolecules* **2010**, *43*, 4937−4942.

(26) Li, Q.; Zhou, H.; Hoyle, C. E. The Effect of Thiol and Ene Structures on Thiol−Ene Networks: Photopolymerization, Physical, Mechanical and Optical Properties. *Polymer* **2009**, *50*, 2237−2245.

(27) Takashima, Y.; Tamura, H.; Hikosaka, T.; Takehana, M. *Google Patents*; 2005. https://patents.google.com/ (accessed Dec 1, 2015).

(28) Ware, T.; Simon, D.; Hearon, K.; Liu, C.; Shah, S.; Reeder, J.; Khodaparast, N.; Kilgard, M. P.; Maitland, D. J.; Rennaker, R. L. Three-Dimensional Flexible Electronics Enabled by Shape Memory Polymer Substrates for Responsive Neural Interfaces. *Macromol. Mater. Eng.* **2012**, *297*, 1193−1202.

(29) Clarson, S. J.; Semlyen, J. A.; Dodgson, K. Cyclic Polysiloxanes: 4. Glass Transition Temperatures of Poly(Phenylmethylsiloxanes). *Polymer* **1991**, *32*, 2823−2827.

DOI: 10.1021/acsami.5b10593
ACS Appl. Mater. Interfaces 2015, 7, 28673−28681

(30) Jeong, G. S.; Baek, D.-H.; Jung, H. C.; Song, J. H.; Moon, J. H.; Hong, S. W.; Kim, I. Y.; Lee, S.-H. Solderable and Electroplatable Flexible Electronic Circuit on a Porous Stretchable Elastomer. *Nat. Commun.* **2012**, *3*, 977.
(31) Voit, W.; Ware, T.; Dasari, R. R.; Smith, P.; Danz, L.; Simon, D.; Barlow, S.; Marder, S. R.; Gall, K. High-Strain Shape-Memory Polymers. *Adv. Funct. Mater.* **2010**, *20*, 162−171.
(32) Zheng, N.; Fang, G.; Cao, Z.; Zhao, Q.; Xie, T. High Strain Epoxy Shape Memory Polymer. *Polym. Chem.* **2015**, *6*, 3046−3053.
(33) Rodríguez, F. J.; Ceballos, D.; Schüttler, M.; Valero, A.; Valderrama, E.; Stieglitz, T.; Navarro, X. Polyimide Cuff Electrodes for Peripheral Nerve Stimulation. *J. Neurosci. Methods* **2000**, *98*, 105−118.
(34) Stieglitz, T.; Schuettler, M.; Meyer, J.-U. Micromachined, Polyimide-Based Devices for Flexible Neural Interfaces. *Biomed. Microdevices* **2000**, *2*, 283−294.
(35) Naples, G. G.; Mortimer, J. T.; Scheiner, A.; Sweeney, J. D. A Spiral Nerve Cuff Electrode for Peripheral Nerve Stimulation. *IEEE Trans. Biomed. Eng.* **1988**, *35*, 905−916.
(36) Kuo, J. T.; Kim, B. J.; Hara, S. A.; Lee, C. D.; Gutierrez, C. A.; Hoang, T. Q.; Meng, E. Novel Flexible Parylene Neural Probe with 3d Sheath Structure for Enhancing Tissue Integration. *Lab Chip* **2013**, *13*, 554−561.

DOI: 10.1021/acsami.5b10593
ACS Appl. Mater. Interfaces 2015, 7, 28673−28681